

# New Insights on the Molecular Mechanism of E-Cadherin mediated Cell-adhesion by Free Energy Calculations

*Fabio Doro,<sup>†,§</sup> Giorgio Saladino,<sup>‡</sup> Laura Belvisi,<sup>†</sup> Monica Civera,<sup>\*,†</sup> and Francesco L. Gervasio<sup>\*,‡</sup>*

<sup>†</sup>Department of Chemistry, University of Milan, Via C. Golgi 19, I-20133, Milan, Italy

<sup>‡</sup>Department of Chemistry and Institute of Structural and Molecular Biology, University College London, 20 Gordon Street, London, UK

## **ABSTRACT**

Three-dimensional domain swapping is an important mode of protein association leading to the formation of stable dimers. Monomers associating via this mechanism mutually exchange a domain to form a homodimer. Classical cadherins, an increasingly important target for anti-cancer therapy, use domain swapping to mediate cell adhesion. However, despite its importance, the molecular mechanism of domain swapping is still debated. Here we study the conformational changes leading to the activation and dimerization via domain swapping of E-cadherin. Using

state-of-the-art enhanced sampling atomistic simulations, we reconstruct its conformational free energy landscape, obtaining the free energy profile connecting the inactive and the active form. Our simulations predict that the E-cadherin monomer populates almost equally the open and the closed form, in agreement with one of the proposed mechanisms, the "selected fit", in which monomers in an active conformational state bind to form the homodimer, in analogy to the conformational selection mechanism often observed in ligand-target binding. Moreover, we find that the open state population is increased in the presence of calcium ions at the extra-cellular boundary, suggesting their possible role as allosteric activators of the conformational change.

## **INTRODUCTION**

Protein-Protein interactions play such a fundamental role in living organisms that proteins are prevalently found in a multimeric aggregation state. Oligomerization can occur in different ways. A common and intriguing mode of association is the so-called three-dimensional (3D) domain swapping,<sup>1</sup> in which oligomers are formed from monomers by exchanging domains. The swapping domains, connected to the remaining part of the protein by a portion called the 'hinge loop', can either be a single secondary structure element, such as a  $\beta$ -strand, or a more extended, multi-structured polypeptide chain. In the monomeric state, the swapping domains are folded inside an acceptor pocket ('closed form'), while in the oligomeric form, they extend onto the corresponding pocket of another protein ('open form').<sup>2</sup>

Among proteins exhibiting 3D domain swapping, cadherins are of particular interest. A large family of calcium-dependent adhesion molecules found at intercellular junctions, cadherins mediate cell-cell adhesion by forming dimers between the N-terminal domains of two proteins localized on adjacent cells.<sup>3</sup> Cadherins pivotal role in cell adhesion explains the involvement of

several of these proteins in tumor progression, making them a promising target for anticancer therapies. For instance E-cadherin, regarded as the prototypical member of classical cadherins, has been reported to play a critical role in the proliferation of various types of cancer.<sup>4,5</sup> For this reason, new anti-cancer agents targeting cadherins are being developed.<sup>6,7</sup>

Classical cadherins consist of an N-terminal extracellular (EC) portion, constituted by five domains (EC1-EC5) rigidified at the interface by calcium ions. Dimerization occurs through the mutual exchange of a highly conserved N-terminal sequence, comprised of the six residues DWVIPP (the “adhesion arm”). In particular, the Trp residue, which in the closed form is inserted in a hydrophobic pocket within the EC1 of the same protein, is docked into the corresponding binding site of the partner protein in the swapped dimer (Figure 1).

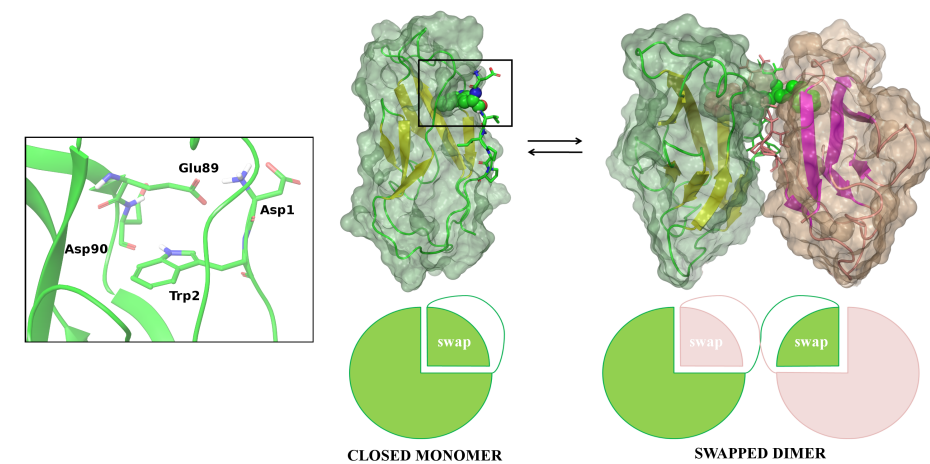


Figure 1. The adhesive binding mechanism of classical cadherins as an example of 3D domain swapping. In the closed form Trp2 is inserted in its hydrophobic pocket while in the swapped dimer it binds to the hydrophobic pocket of another cadherin molecule (pdb code: 3Q2V). On the left, the salt bridge formed in the closed monomer between the side chain of Glu89 and the N-terminus  $\text{NH}_3^+$  of Asp1 can also be appreciated. Structure for the closed monomer derives from our simulations.

Clusterization of such swap dimers at the cellular interface leads to the formation of organized oligomers.<sup>8</sup>

In the last decade, experimental data suggesting the existence of two possible 3D swapping mechanisms, a selected fit and an induced fit pathway (Figure S1), have been reported.<sup>9-13</sup> The former mechanism assumes that monomers in the closed form first undergo a conformational change leading to the active open form and only in a second step they bind each other. According to the induced fit mechanism, the dimerization occurs via an intermediate complex, the ‘encounter complex’, that lowers the energy barrier required for the swap dimer formation. The mechanism through which the two monomers form the encounter complex, as well as the conformational changes that lead to the swap dimer from the encounter complex, are currently unknown. Moreover, the encounter complex has not been yet structurally characterized, although it is usually associated with the so-called X-dimer, an alternative dimer conformation which is formed when swap-impaired cadherins aggregate.<sup>14</sup> However, it is worth noting that mutations that prevent the formation of the X-dimer do not alter the ability of classical cadherins to form swap dimers.<sup>12</sup> This suggests the existence of at least two alternative mechanisms of dimerization of classical cadherins. Herein, we investigate the selected fit hypothesis by reconstructing the free energy profile of the conformational transition of the type I E-cadherin monomer, from its closed inactive state to the open form. This represents the first step of the supposed two-step selected fit mechanism. Only if the free energy and population of the two forms are comparable a selected fit mechanism would be possible.

The timescale involved in the swapping mechanism prevents the observation of cadherins conformational changes with conventional Molecular Dynamics (MD) simulations. For this

reason we used a state-of-the-art enhanced sampling technique, namely a combination of parallel tempering and metadynamics PT-MetaD<sup>15</sup>.

This method has been successfully used to converge the multi-dimensional free energy landscape associated with the folding of small proteins,<sup>15,16</sup> complex conformational changes in protein kinases<sup>17,18</sup> and the folding and oligomerization of fibrin foldon domains.<sup>19</sup> In the Well Tempered Ensemble (WTE) methodology, used in the present study, a static bias on the potential energy of the system is applied in the PT-MetaD simulation, with the purpose of increasing the energy overlap between replicas and thus enhancing the sampling efficacy.<sup>20</sup>

Since calcium ions modulate cadherins biological activity, we also investigated their role in the E-cadherin monomer closed-to-open transition. First, we assessed the stability of the EC1-EC2 domain with and without calcium ions, by performing two 100 ns unbiased MD simulations (Figure S2). As also shown in a previous work,<sup>21</sup> absence of Ca<sup>2+</sup> ions at the EC boundary causes the system to lose its linearity, which is needed by the cadherin in order to carry out its function. As a consequence, the systems for the subsequent biased simulations were set up as follows: (1) EC1 domain with no Ca<sup>2+</sup> ions and (2) EC1-EC2 domain containing three Ca<sup>2+</sup> ions at the inter-domain boundary. By analyzing the free energy profiles of the two systems, we extrapolated the impact of the calcium ions in favoring the E-cadherin conformational change.

## EXPERIMENTAL SECTION

In a recent comparative study<sup>22</sup> CHARMM22\*<sup>23</sup> and Amber99SB\*-ILDN<sup>23,24</sup> were ranked among the best protein force fields, both reproducing a wide range of experimental data. More recently, we compared the performance of these two force-fields together with PT-metaD in reproducing the conformational energy landscape of proline isomerase.<sup>25</sup> Both were able to

reproduce the experimental free energy difference between the major and minor conformers, but the simulations performed with CHARMM22\* showed an enhanced flexibility, in agreement with previous observations that it might be better at predicting the folding kinetics of small proteins. Thus, here we performed our simulations using the CHARMM22\* force field together with GROMACS 4.5.5<sup>26</sup> and PLUMED 1.3.<sup>27</sup> We obtained the initial coordinates from the X-ray structure (PDB id: 1FF5<sup>28</sup>) of an E-cadherin X-dimer, which is the only available experimental structure in a closed conformation. Then, we constructed two independent monomeric systems in the closed form, EC1 containing residues 1-99 and no calcium ions, and EC1-EC2 containing residues 1–215, three Ca<sup>2+</sup> ions at the extracellular boundary and a fourth calcium ion at the end of EC2. The first system was solvated in a rhombic dodecahedron box adding 9253 TIP3P water molecules and the second was solvated in a triclinic box adding 15136 TIP3P water molecules. Calcium ions were modeled following Bjelkmar and co-workers.<sup>29</sup> We started our simulations by first minimizing the systems using a steepest descent algorithm. We then performed an equilibration in two steps: first, we simulated the systems for 1 ns at 300 K in an NVT ensemble, using the velocity-rescale thermostat<sup>31</sup> and positional restraint on the proteins, then, a 10 ns NPT simulation using a Parrinello-Rahman barostat<sup>32</sup> with no restraint concluded the equilibration. Particle Mesh Ewald method was used for treating long range electrostatics, using a cutoff of 10 Å. A time step of 2 fs was used for all simulations.

To run in the WTE ensemble, we first performed a preliminary PT-MetaD<sup>15,16</sup> run with four replicas of each system using the potential energy as the only CV, according to the original WTE article.<sup>20</sup> Temperatures for each replica were 300 K, 330 K, 362 K and 398 K. Gaussians having height of 4.0 kJ/mol were added every 500 MD steps. Exchanges among replicas were attempted every 250 MD steps. The average exchange probability was around 30% for both systems. The

obtained bias on the potential energy was kept fixed during the following PT-MetaD run, thus running in the WTE ensemble.

The production run for each system was performed using the following three Collective Variables: the distance between His79 C $\alpha$  and the centroid of the indole moiety in Trp2 (CV1), needed to discriminate between closed and open conformations, the improper dihedral defined by two heavy atoms in the Trp indole ring and the centroids of two sets of C $\alpha$  atoms in the  $\beta$ -strand regions 73-80 and 92-97 (CV2), which well describes the orientation of Trp2 indole moiety inside the cavity, and a Contact Map counting the number of selected contacts between the adhesion arm and its pocket (CV3). The Contact Map was selected on the basis of the cluster analysis of snapshots of closed, intermediate and open forms of E-cadherin taken from short MetaD simulations. Analysis of the different atom distances between the hydrophobic pocket and the opening arm, in the three forms, allowed us to define a CV describing the path along which the conformational change occurs (see Figure S3 and Table S1 for a depiction of the CVs). Gaussians of height 1.3 kJ/mol were added every 500 MD steps, using a bias factor of 12 for both systems. Simulations ran in NVT conditions with a time step of 2 fs until all the interesting regions in the CV space were fully explored. To assess the convergence of the simulations, we applied a recently developed reweighting algorithm by Tiwary and Parrinello<sup>33</sup> and obtained a time-independent estimate of the free energy (Figure S4 for the projection of the free energy onto CV1), by which we calculated the error on the free energy differences. In addition, we independently rerun the EC1 system and verified that the reconstructed free energies converge to the same profile (Figure S5).

Conformations belonging to each minimum were extracted and clustered using the `g_cluster` GROMACS tool with a single linkage method and a cut-off of 1 Å over the RMS distance computed on EC1 C $\alpha$  atoms.

## RESULTS

The conformational free energies surfaces projected onto two relevant coordinates, namely the His79-Trp2 distance (CV1) and the orientation of the Trp2 indole moiety with respect to the protein backbone (CV2), are shown in Figure 2.

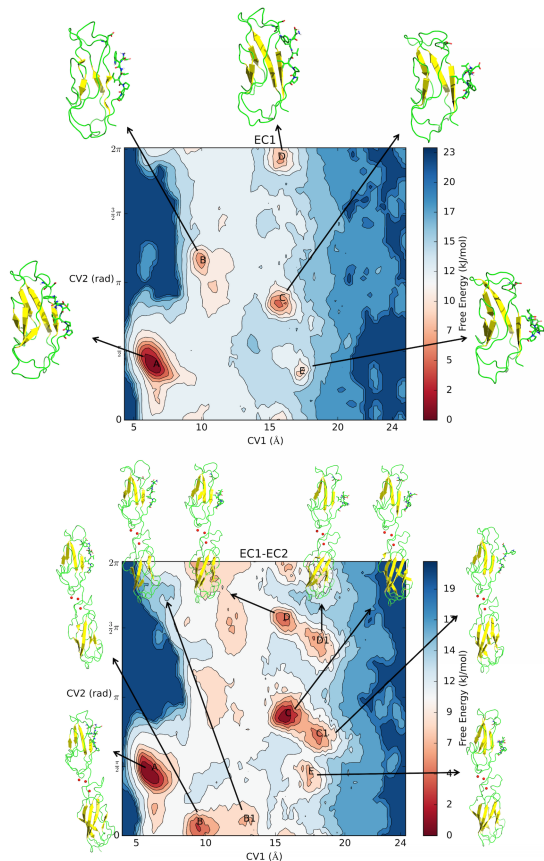


Figure 2. Free energy surfaces (at 300K) associated with the closed-to-open conformational transition of EC1 (top) and EC1-EC2 (bottom) E-cadherin, projected on the CV1 (Trp2-His79 distance) and CV2 (Trp2 orientation) space. The most representative structures of each local minimum, obtained from cluster analysis, are reported. Contour lines are drawn with a stride of 2 kJ/mol.

In both systems, the global minimum corresponds to a closed conformation (minimum A in both maps) with the Trp2 side chain being firmly docked into its hydrophobic pocket and forming an hydrogen bond with the Asp90 backbone, as observed in the X-ray structure.

However, while the EC1-EC2 complex is characterized by a salt bridge between the Asp1 N-terminus and the Glu89 side chain (99% of the structures), the EC1 alone formed this interaction only in the 47% of the structures (in the remaining 53% the Asp1 N-terminus is exposed to the solvent). Only at higher energies (by at least 8 kJ/mol) we could observe closed conformations in which the indole moiety plane is differently oriented inside the pocket and either points towards Glu89 (90 degrees rotation of the indole plane with respect to the structures representing the global minimum) or Lys25 (180 degrees rotation). These conformations, characterized by a loose Asp1-Glu89 salt bridge are likely to represent metastable closed-like forms, with weaker interactions between the adhesion arm and the hydrophobic pocket. These findings regarding the closed form of both systems are in agreement with the hypothesis of an open/closed state equilibrium in which the Trp2 indole exits the cavity and re-enters it with a different orientation.

The other energy minima found on the maps represent different open states of EC1 (Figure 2, up) and EC1-EC2 (Figure 2, down). Indeed, the Trp2 side chain is relatively free to move in solution and so it can adopt different conformations. The presence of calcium ions at the EC boundary seems to enhance this entropy-driven process, since in EC1-EC2 we observe a broader selection of open conformations. In both cases the open forms adopt different positions of the indole Trp2 ring with respect to the protein principal axis at the same value of the Trp2 distance from binding pocket. In fact, considering only the CV1 values (see also Figure S6), both systems showed two major open states, one located at CV1 values around 10 Å, in which the adhesion arm tends to adhere to the rest of the protein in order to minimize solvent exposure (as in minima B of Figure 2) and another, energetically more favored, located at CV1 values around 16 Å, with the adhesion arm completely exposed to the solvent (minima C, D and E of Figure 2). It is worth noting that the most representative structures of EC1-EC2 belonging to the minimum C1

superimpose well to the open conformation of the X-ray swap dimer structure (PDB id: 3Q2V,<sup>8</sup> C $\alpha$  RMSD = 0.76 Å, Figure S7). In EC1, the energy difference between the main open and closed minima is  $5.4 \pm 1.5$  kJ/mol, while in EC1-EC2 the minimum located at 16 Å is isoenergetic (with an estimated sampling error of 0.6 kJ/mol) to the closed form. The energetic barrier for the closed/open transition for the EC1-EC2 and the EC1 systems,  $14 \pm 4$  kJ/mol, and  $16 \pm 4$  kJ/mol, respectively, are within the sampling error. The larger sampling error on the energy barriers is due to the nature of the PT-metaD approach.<sup>15</sup> The above-mentioned energy values for the closed/open barrier can be used to estimate the crossing rate between the two states. Due to the diffusive nature of the dynamics, we followed the approach of Juraszek and co-workers<sup>34</sup> and estimated a transmission coefficient  $k$  of  $\sim 10^{-3}$  that corrects for the correlated recrossings at the transition state. This gives us an estimate for the rates of 56 – 1400 ns (for EC1) and 25 - 622 ns (for EC1-EC2). At both ends of the predicted range the kinetics are very fast. The fast inter-conversion rate between open and closed forms is in agreement with a selected fit mechanism. It is worth noting that in cadherin 8, a type II cadherin, by using NMR dispersion relaxation techniques, Miloushev and co-workers<sup>13</sup> have detected the existence in solution of the open form.

Projection of the free energy on a 2D map using CV1 and CV3 allowed a characterization of the arm opening mechanism. The third collective variable (CV3) maps the atomic contacts between the adhesion arm and the hydrophobic pocket (Table S1): CV3 values around 3 represent the starting closed conformation, while for values around 1, the adhesion arm is completely exposed to the solvent, representing a fully open state.

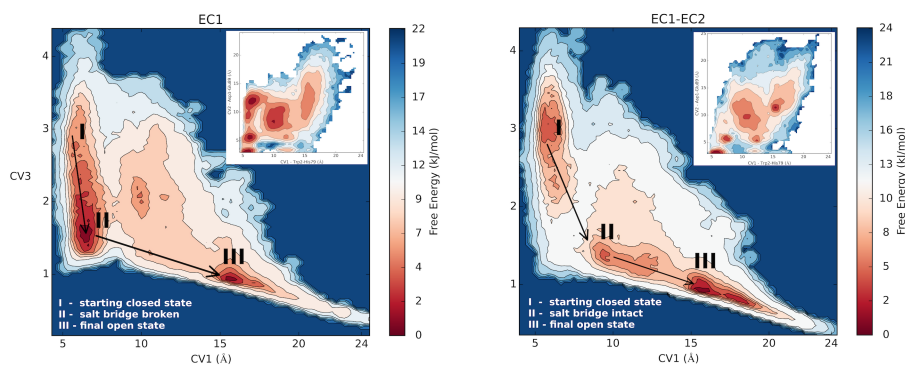


Figure 3. Reconstructed free energies projected on a 2D surface using CV1 and CV3 for EC1 (left) and EC1-EC2 (right) E-cadherin monomer. Isolines are drawn every 2.0 kJ/mol. The salt bridge refers to the electrostatic interaction between Asp1-NH<sub>3</sub><sup>+</sup> and Glu89 side chain. In EC1, breaking of the salt bridge (I to II) precedes the exit of Trp2 from the pocket (II to III) while in EC1-EC2 the indole moiety first leaves the hydrophobic pocket (I to II) and only in a second step the electrostatic interaction gets broken (II to III). We also used a reweighting algorithm to directly project the free energy on the Asp1-NH<sub>3</sub><sup>+</sup> – Glu89 salt bridge distance (on the Y-axis) and on the Trp2 – His79 distance (shown as insets in the top right of each map).

In Figure 3 we reported the free energy surface as a function of CV1 and CV3. From the analysis of the structures belonging to each minimum we found that the two systems followed distinct opening pathways. In EC1 (Figure 3, left), the first step is characterized by the disruption of the salt bridge (I to II, CV3 from 3 to 2) with the Trp2 side chain docked onto its pocket, and only in the second step Trp2 leaves the hydrophobic pocket and exposes the indole moiety to the solvent (II to III, CV3 from 2 to 1). A conformational equilibrium was in fact observed for the closed form of EC1 (minimum A of Figure 2, up) where the two most representative conformations differ only by the presence of the salt bridge. For this system, it seems that the lacking of calcium ions facilitates the breaking of the salt bridge but not the opening of the arm.

In EC1-EC2 (Figure 3, right, from I to II), first the Trp2 indole moiety moves towards the solvent, while maintaining the salt bridge between the Glu89 side chain and Asp1 (CV3 from 3 to 1.5). At this point, the adhesion arm is still relatively close to the rest of the protein, and only in the second step, when the salt bridge is broken, it is able to fully open (II to III, CV3 from 1.5 to 1). This pathway is in agreement with what we observed during the simulations. In fact, in the first part of the simulation the Trp2 side chain exited and re-entered the hydrophobic pocket several times without breaking the salt bridge. Only when the salt bridge is broken, these events become less probable. Moreover, this analysis shows that the major contribution to the interaction energy of the adhesive arm with the pocket seems to derive from the salt bridge between the Asp1 and the Glu89, two highly conserved residues in all classical cadherins. The same conclusions regarding the two different pathways can be drawn if one observes the free energies projected directly on the salt bridge distance (Figure 3, insets). To extract the unbiased distribution for the Asp1-NH<sub>3</sub><sup>+</sup> – Glu89 distance, we used the reweighting algorithm developed by Bonomi and co-workers.<sup>35</sup> Only in EC1 there is a well-defined minimum at CV values (6 Å – 12 Å), corresponding to a closed conformation with a broken salt bridge. Vendome and co-workers postulated that calcium ions could introduce some strain in the adhesive arm and the release of such strain could be the driving force behind the opening of the arm.<sup>36</sup> Our findings are in agreement with such an hypothesis — when calcium ions are present, strain is first released by exposing Trp2 to the solvent, followed by the full opening of the arm — but also introduce the N-terminus–Glu89 salt bridge as a key interaction in the opening path.

## CONCLUSIONS

Our simulations predict that the EC1-EC2 E-cadherin monomer, in the presence of calcium ions, significantly populates both open and closed forms, which are almost iso-energetic. This observation is in agreement with the proposed selected fit mechanism. Although recent studies have suggested for E-cadherin an induced fit mechanism<sup>11</sup>, when we attempted protein-protein docking<sup>37</sup> using both the major and minor states of the EC1-EC2 E-cadherin system we could not reproduce a viable X-dimer conformation (Table S2). On the contrary, the low free energy penalty and fast kinetics that we predict for the system is strongly suggestive of a conformational selection mechanism. What is more, we are able for the first time to provide a detailed characterization of the conformational transition of the E-cadherin monomer that was postulated to exist based on the proposed selected fit mechanism. By using a state-of-the-art enhanced sampling algorithm, we obtained a fully converged multidimensional conformational free energy landscape describing the arm opening transition and intermediate metastable states. These states might provide a starting point for the design of new inhibitors and perhaps lead to anti-cancer agents, as well as help identify the encounter complex structure, a necessary step in order to attempt an atomic resolution description of the alternate induced fit mechanism of cadherins dimerization. Finally, our simulations confirm that calcium ions favor the opening of the arm by stabilizing the open form.

## ASSOCIATED CONTENT

### **Supporting Information.**

Dimerization proposed mechanisms, trajectory analysis for unbiased simulations, CV1-CV2 description, Contact Map (CV3) description, free energy profiles projected on the CV1 with

error estimation, docking results for EC1-EC2. This material is available free of charge via the Internet at <http://pubs.acs.org>.

## **AUTHOR INFORMATION**

### **Corresponding Authors**

\*Email: [monica.civera@unimi.it](mailto:monica.civera@unimi.it)

\*Email: [f.l.gervasio@ucl.ac.uk](mailto:f.l.gervasio@ucl.ac.uk)

### **Present Addresses**

§Structural Biology and NMR laboratory, Department of Biology, University of Copenhagen, Ole Maaløes Vej 5, 2200 Copenhagen N, Denmark

### **Notes**

The authors declare no competing financial interest.

## **ACKNOWLEDGMENT**

We acknowledge HPC-Europa2 Programme (Application number 1024) and MIUR (FIRB RBF088ITV project) for financial support. We also thank the University of Milan for PhD Fellowship to Fabio Doro and CINECA for computing facilities.

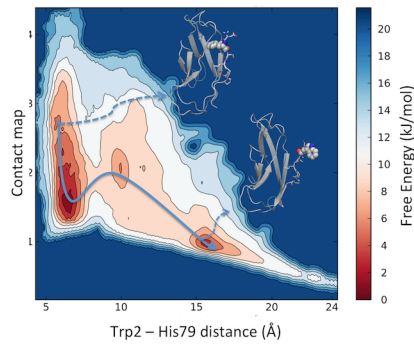
## **REFERENCES**

- (1) Bennett, M. J.; Schlunegger, M. P.; Eisenberg, D. 3D Domain Swapping: A Mechanism for Oligomer Assembly. *Protein Sci.* **1995**, *4*, 2455–2468.
- (2) Gronenborn, A. M. Protein Acrobatics in Pairs--Dimerization via Domain Swapping. *Curr. Opin. Struct. Biol.* **2009**, *19*, 39–49.

- (3) Leckband, D.; Sivasankar, S. Cadherin Recognition and Adhesion. *Curr. Opin. Cell Biol.* **2012**, *24*, 620–627.
- (4) Berx, G.; van Roy, F. Involvement of Members of the Cadherin Superfamily in Cancer. *Cold Spring Harb. Perspect. Biol.* **2009**, *1*, a003129.
- (5) De Santis, G.; Miotti, S.; Mazzi, M.; Canevari, S.; Tomassetti, A. E-Cadherin Directly Contributes to PI3K/AKT Activation by Engaging the PI3K-p85 Regulatory Subunit to Adherens Junctions of Ovarian Carcinoma Cells. *Oncogene* **2009**, *28*, 1206–1217.
- (6) Blaschuk, O. W.; Devemy, E. Cadherins as Novel Targets for Anti-Cancer Therapy. *Eur. J. Pharmacol.* **2009**, *625*, 195–198.
- (7) Doro, F.; Colombo, C.; Alberti, C.; Arosio, D.; Belvisi, L.; Casagrande, C.; Fanelli, R.; Manzoni, L.; Parisini, E.; Piarulli, U.; Luison, E.; Figini, M.; Tomassetti, A.; Civera, M. Computational Design of Novel Peptidomimetic Inhibitors of Cadherin Homophilic Interactions. *Org. Biomol. Chem.* **2015**, *13*, 2570–2573.
- (8) Harrison, O. J.; Jin, X.; Hong, S.; Bahna, F.; Ahlsen, G.; Brasch, J.; Wu, Y.; Vendome, J.; Felsovalyi, K.; Hampton, C. M.; Troyanovsky, R. B.; Ben-Shaul, A.; Frank, J.; Troyanovsky, S. M.; Shapiro, L.; Honig, B.; Sergey, M. The Extracellular Architecture of Adherens Junctions Revealed by Crystal Structures of Type I Cadherins. *Structure* **2011**, *19*, 244–256.
- (9) Brasch, J.; Harrison, O. J.; Honig, B.; Shapiro, L. Thinking Outside the Cell: How Cadherins Drive Adhesion. *Trends Cell Biol.* **2012**, *22*, 299–310.
- (10) Sivasankar, S.; Zhang, Y.; Nelson, W. J.; Chu, S. Characterizing the Initial Encounter Complex in Cadherin Adhesion. *Structure* **2009**, *17*, 1075–1081.
- (11) Li, Y.; Altorelli, N. L.; Bahna, F.; Honig, B.; Shapiro, L.; Palmer, A. G. Mechanism of E-Cadherin Dimerization Probed by NMR Relaxation Dispersion. *Proc. Natl. Acad. Sci. U. S. A.* **2013**, *110*, 16462–16467.
- (12) Harrison, O. J.; Bahna, F.; Katsamba, P. S.; Jin, X.; Brasch, J.; Vendome, J.; Ahlsen, G.; Carroll, K. J.; Price, S. R.; Honig, B.; Shapiro, L. Two-Step Adhesive Binding by Classical Cadherins. *Nat. Struct. Mol. Biol.* **2010**, *17*, 348–357.
- (13) Miloushev, V. Z.; Bahna, F.; Ciatto, C.; Ahlsen, G.; Honig, B.; Shapiro, L.; Palmer, A. G. Dynamic Properties of a Type II Cadherin Adhesive Domain: Implications for the Mechanism of Strand-Swapping of Classical Cadherins. *Structure* **2008**, *16*, 1195–1205.
- (14) Ciatto, C.; Bahna, F.; Zampieri, N.; VanSteenhouse, H. C.; Katsamba, P. S.; Ahlsen, G.; Harrison, O. J.; Brasch, J.; Jin, X.; Posy, S.; Vendome, J.; Ranscht, B.; Jessell, T. M.; Honig, B.; Shapiro, L. T-Cadherin Structures Reveal a Novel Adhesive Binding Mechanism. *Nat. Struct. Mol. Biol.* **2010**, *17*, 339–347.

- (15) Bussi, G.; Gervasio, F. L.; Laio, A.; Parrinello, M. Free-Energy Landscape for Beta Hairpin Folding from Combined Parallel Tempering and Metadynamics. *J. Am. Chem. Soc.* **2006**, *128*, 13435–13441.
- (16) Deighan, M.; Bonomi, M.; Pfendtner, J. Efficient Simulation of Explicitly Solvated Proteins in the Well-Tempered Ensemble. *J. Chem. Theory Comput.* **2012**, *8*, 2189–2192.
- (17) Lovera, S.; Sutto, L.; Boubeva, R.; Scapozza, L.; Dölker, N.; Gervasio, F. L. The Different Flexibility of c-Src and c-Abl Kinases Regulates the Accessibility of a Druggable Inactive Conformation. *J. Am. Chem. Soc.* **2012**, *134*, 2496–2499.
- (18) Sutto, L.; Gervasio, F. L. Effects of Oncogenic Mutations on the Conformational Free-Energy Landscape of EGFR Kinase. *Proc. Natl. Acad. Sci. U. S. A.* **2013**, *110*, 10616–10621.
- (19) Barducci, A.; Bonomi, M.; Prakash, M. K.; Parrinello, M. Free-Energy Landscape of Protein Oligomerization from Atomistic Simulations. *Proc. Natl. Acad. Sci. U. S. A.* **2013**, *110*, E4708–E4713.
- (20) Bonomi, M.; Parrinello, M. Enhanced Sampling in the Well-Tempered Ensemble. *Phys. Rev. Lett.* **2010**, *104*, 190601.
- (21) Cailliez, F.; Lavery, R. Cadherin Mechanics and Complexation: The Importance of Calcium Binding. *Biophys. J.* **2005**, *89*, 3895–3903.
- (22) Lindorff-Larsen, K.; Maragakis, P.; Piana, S.; Eastwood, M. P.; Dror, R. O.; Shaw, D. E. Systematic Validation of Protein Force Fields against Experimental Data. *PLoS One* **2012**, *7*, e32131.
- (23) Piana, S.; Lindorff-Larsen, K.; Shaw, D. E. How Robust Are Protein Folding Simulations with Respect to Force Field Parameterization? *Biophys. J.* **2011**, *100*, L47–L49.
- (24) Lindorff-Larsen, K.; Piana, S.; Palmo, K.; Maragakis, P.; Klepeis, J. L.; Dror, R. O.; Shaw, D. E. Improved Side-Chain Torsion Potentials for the Amber ff99SB Protein Force Field. *Proteins* **2010**, *78*, 1950–1958.
- (25) Papaleo, E.; Sutto, L.; Gervasio, F. L.; Lindorff-Larsen, K. Conformational Changes and Free Energies in a Proline Isomerase. *J. Chem. Theory Comput.* **2014**, *10*, 4169–4174.
- (26) Pronk, S.; Páll, S.; Schulz, R.; Larsson, P.; Bjelkmar, P.; Apostolov, R.; Shirts, M. R.; Smith, J. C.; Kasson, P. M.; van der Spoel, D.; Hess, B.; Lindahl, E. GROMACS 4.5: A High-Throughput and Highly Parallel Open Source Molecular Simulation Toolkit. *Bioinformatics* **2013**, *29*, 845–854.
- (27) Bonomi, M.; Branduardi, D.; Bussi, G.; Camilloni, C.; Provasi, D.; Raiteri, P.; Donadio, D.; Marinelli, F.; Pietrucci, F.; Broglia, R. A.; Parrinello, M. PLUMED: A Portable Plugin

- for Free-Energy Calculations with Molecular Dynamics. *Comput. Phys. Commun.* **2009**, *180*, 1961–1972.
- (28) Pertz, O.; Bozic, D.; Koch, A. W.; Fauser, C.; Brancaccio, A.; Engel, J. A New Crystal Structure, Ca<sup>2+</sup> Dependence and Mutational Analysis Reveal Molecular Details of E-Cadherin Homoassociation. *EMBO J.* **1999**, *18*, 1738–1747.
- (29) Bjelkmar, P.; Larsson, P.; Cuendet, M. A.; Hess, B.; Lindahl, E. Implementation of the CHARMM Force Field in GROMACS: Analysis of Protein Stability Effects from Correction Maps, Virtual Interaction Sites, and Water Models. *J. Chem. Theory Comput.* **2010**, *6*, 459–466.
- (30) Baştuğ, T.; Kuyucak, S. Energetics of Ion Permeation, Rejection, Binding, and Block in Gramicidin A from Free Energy Simulations. *Biophysical Journal*, 2006, *90*, 3941–3950.
- (31) Bussi, G.; Donadio, D.; Parrinello, M. Canonical Sampling through Velocity Rescaling. *J. Chem. Phys.* **2007**, *126*, 014101.
- (32) Parrinello, M.; Rahman, A. Polymorphic Transitions in Single Crystals: A New Molecular Dynamics Method. *J. Appl. Phys.* **1981**, *52*, 7182.
- (33) Tiwary, P.; Parrinello, M. A Time-Independent Free Energy Estimator for Metadynamics. *J. Phys. Chem. B* **2015**, *119*, 736–742.
- (34) Juraszek, J.; Saladino, G.; van Erp, T. S.; Gervasio, F. L. Efficient Numerical Reconstruction of Protein Folding Kinetics with Partial Path Sampling and Pathlike Variables. *Phys. Rev. Lett.* **2013**, *110*, 108106.
- (35) Bonomi, M.; Barducci, a; Parrinello, M. Reconstructing the Equilibrium Boltzmann Distribution from Well-Tempered Metadynamics. *J. Comput. Chem.* **2009**, *30*, 1615–1621.
- (36) Vendome, J.; Posy, S.; Jin, X.; Bahna, F.; Ahlsen, G.; Shapiro, L.; Honig, B. Molecular Design Principles Underlying B-Strand Swapping in the Adhesive Dimerization of Cadherins. *Nat. Struct. Mol. Biol.* **2011**, *18*, 693–700.
- (37) Kozakov, D.; Brenke, R.; Comeau, S. R.; Vajda, S. PIPER: An FFT-Based Protein Docking Program with Pairwise Potentials. *Proteins Struct. Funct. Bioinforma.* **2006**, *65*, 392–406.



The free energy profile of E-cadherin conformational transition has been reconstructed using atomistic simulations. Both the inactive and active conformations coexist in solution, suggesting the possibility of a selected fit pathway for this class of domain swapping proteins. Calculations also show that calcium ions located far from the exchanging arm may act as allosteric activators.